Immunity, Vol. 20, 231–242, February, 2004, Copyright ©2004 by Cell Press

Developmentally Distinct Th Cells Control Plasma Cell Production In Vivo

Louise J. McHeyzer-Williams and Michael G. McHeyzer-Williams*
Department of Immunology
The Scripps Research Institute
10550 North Torrey Pines Road
La Jolla, California 92037

Summary

Differential Ly6C expression identifies a major phenotypic division in CD44^{lo}CD62L^{hi}CD4^{+} Th cells. Using two separate models of single subset adoptive transfer, we demonstrate the unique capacity of Ly6C^{hi} Th cells to promote antigen-specific plasma cell production in vivo. In contrast, both compartments support germinal center formation and proliferate to equivalent levels upon TCR triggering in vivo and in vitro. Developmentally, CD4^{+}CD8^{-} thymocytes leave the thymus expressing low levels of Ly6C; 3 days later ~50% stably upregulate Ly6C without cell division or TCR engagement in the periphery. Interestingly, antigen-specific Th cell clonotypes unevenly assort into these peripheral compartments, creating separate TCR repertoires that underpin peripheral functional diversity. Taken together, these data reveal a developmentally distinct Ly6C^{hi} naive Th cell compartment subspecialized to regulate plasma cell production in vivo.

Introduction

Steady-state preimmune lymphocytes are organized into multiple functionally subspecialized cellular compartments. In the B cell compartment, B1 B cells, marginal zone (MZ) B cells, and follicular (FO) IgD^{+}IgM^{+} B cells represent known functionally distinct B cell compartments (McHeyzer-Williams and Ahmed, 1999; McHeyzer-Williams, 2003). Within αβ T cells, the imprinting of MHC restriction broadly assorts peripheral T cell function across CD8^{+} cytotoxic T cells and CD4^{+} T cells (Woodland and Dutton, 2003). The CD4 compartment contains a suppressor-helper cell division based on peripheral function. Suppressor T cells negatively regulate the peripheral response to self-antigens and help to maintain immune tolerance (Sakaguchi et al., 1995). In contrast, helper T cells positively regulate CD8 T cell responses and B cell responses to foreign antigen. These helper T cells have substantial impact on the quality of primary effector immune responses and the subsequent development of long-term protective immunity. Thus, the adaptive immune system preassorts lymphocytes into multiple layers based on antigen receptor expression and predetermined functional capacity.

Helper T cell regulation of B cell immunity involves a multitude of different effector Th functions. At the peak of clonal expansion in vivo, antigen-specific Th cells express a range of cell surface phenotypes (McHeyzer-Williams and Davis, 1995; McHeyzer-Williams et al., 1999), distinct physiological properties (Bikah et al., 2000; Panus et al., 2000), and the capacity to produce different sets of cytokines (Bikah et al., 2000; Panus et al., 2000). These effector Th cells regulate the emergence of short-lived plasma cells and help to establish the germinal center reaction. Short-lived plasma cells secrete germline-encoded specific antibody that enhances the rapid clearance of antigen. This rapid effector activity is critical to the immediate survival of the host in response to many infectious agents. In contrast, the germinal center reaction underpins memory B cell development and is a more delayed response to antigen. This dynamic microenvironment couples clonal expansion and BCR hypermutation with affinity-based selection to produce antigen-specific B cell memory (Jacob et al., 1991; McHeyzer-Williams et al., 1991, 1993). These rapid and delayed B cell fates are initiated and controlled in vivo by antigen-specific Th cells in ways that are still poorly understood.

Murine Ly-6 molecules are a family of low molecular weight (12–20 kDa) glycosylphosphatidyl-inositol (GPI) anchored cell surface glycoproteins (Ly6A/E [Sca-1/TSA-1], Ly6B, Ly6C, Ly6d [ThB], Ly6F, Ly6G [GR-1], Ly6H, Ly6I, and TSA-2 [Sca-2]) (Rock et al., 1989). While they have been useful indicators of developmental progression in the hematopoietic system (Spangrude et al., 1988), little is known of their function. Ly6 molecules are involved in cellular interactions (Bamezai and Rock, 1995) and T cell activation (Walunas et al., 1995; Tough et al., 1996), and have been associated with lineage commitment in multipotential stem cells (Spangrude et al., 1988). These GPI-anchored proteins are resident in lipid raft membrane microdomains (Bohuslav et al., 1993) with reported capacity to impact TCR signal transduction (Malek et al., 1986; Lee et al., 1994). Ly6 molecules are implicated in cell fate decisions through specific receptor-ligand interactions (Apostolopoulos et al., 2000; Pflugh et al., 2002) that remain poorly resolved for most members of this large family of molecules.

More specifically, Ly6C is expressed to variable levels on T cells. Small populations of thymocytes express Ly6C, but it is most prevalent on double-negative (DN) thymocytes (Schlueter et al., 1997). CD22 may act as a ligand for this member of the family; however, Ly6A/E binds more strongly than Ly6C (Pflugh et al., 2002). Ly6C expression is markedly elevated on activated CD8^{+} T cells (Walunas et al., 1995; Tough et al., 1996) but has a complex distribution pattern on naive CD4 cells with variation in allotype and expression across different strains of mice (Schlueter et al., 1997). In the Ly6.2 strains of mice (C57BL/6, DBA/2, and B10.BR), a substantial fraction of Th cells express Ly6C in the periphery. Therefore, differential Ly6C expression can divide the naive Th cell compartment, but the basis for this division and its impact on Th cell function remains unknown.

In the current study, we focus on animals with a substantial Ly6C^{hi} and Ly6C^{lo} division in the naive peripheral Th cell compartment. We demonstrate distinct func-

*Correspondence: mcheyzer@scripps.edu

tional potentials in two separate adoptive transfer models of antigen-specific immunity. This peripheral cell fate decision appears predetermined in the thymus and does not require clonal expansion or TCR engagement in the periphery. In contrast, TCR specificity does assort unevenly across the two peripheral Ly6C subsets, implicating self-pMHC II as a major determinant in this thymic developmental event.

Results

Ly6C Expression Divides the Preimmune CD4 Th Cell Compartment

The vast majority of $CD4^+CD8^-$ (96 ± 0.8%) and $CD8^+CD4^-$ (92 ± 0.7%) single-positive (SP) thymocytes in nontransgenic B10.BR mice express low levels of Ly6C (Figures 1A and 1B; mean fluorescence intensity; MFI 13 ± 3 and 11 ± 1, respectively). In the periphery, 50 ± 1.4% of naive $CD4^+CD8^-$ Th cells (Figures 1A and 1B, upper panels; naive defined as $CD44^{lo}$ in this case; also true for $CD62L^{hi}$ Th cells and $CD69^{lo}$ Th cells) appear with substantially higher levels of Ly6C (35-fold increase from thymus levels; MFI 460 ± 13), while the other half remain low for Ly6C (2-fold increase on thymus levels; MFI 29 ± 5). The same Ly6C distribution is found in lymph nodes (LN) and spleen.

A similar but exaggerated trend is seen in the $CD8^+CD4^-$ T cells where the $Ly6C^{hi}$ cells in the periphery have increased levels 130-fold above that seen in the thymus and the $Ly6C^{lo}$ remain similarly low (Figures 1A and 1B, lower panels). In this case, most of the $Ly6C^{hi}$ $CD8^+$ cells also express high levels of CD44 (data not shown), consistent with upregulation of Ly6C upon antigen encounter. In contrast, virtually all $CD4^+CD44^{hi}$ Th cells express low levels of Ly6C (Figure 1C, second panel). Furthermore, upon immunization with the model antigen pigeon cytochrome C (PCC) (McHeyzer-Williams and Davis, 1995; McHeyzer-Williams et al., 1999), all PCC-specific Th cells express low levels of Ly6C as early as day 3 after priming (data not shown) and remain $Ly6C^{lo}$ thereafter (into the late primary and after antigen recall; data not shown). Therefore, upregulation of Ly6C in the CD4 Th cell compartment is not associated with antigen experience and is most likely a preimmune consequence of T cell development.

There is a 5-fold difference in Ly6C mRNA levels (15000 ± 1800 and 2900 ± 52 $Ly6C^{hi}$ and $Ly6C^{lo}$, respectively, using Affymetrix Microarray Analysis; data not shown), suggesting that the 16-fold difference in protein expression (using MFI from Figure 1A) is further regulated at the transcriptional and posttranscriptional level. A similar difference in mRNA is seen for another Ly6 family member, Ly6A/E (12000 ± 1300 versus 5000 ± 610, respectively), also found at the protein level (MFI, 2090 ± 89 and 923 ± 29 in $Ly6C^{hi}$ and $Ly6C^{lo}$ naive Th cells, respectively; $p = 0.0002$) (Figure 1D). Two other important modulators of TCR responsiveness, CD5 and CD28, are significantly different at the mRNA level between these two subsets ($p = 0.02$ and $p = 0.007$, respectively) (data not shown). CD5 protein expression is also significantly different between the two Th cell subsets (Figure 1D; $p = 0.002$). Hence, naive Th cells divided in vivo across one phenotypic variation exhibit a number of other differences at both mRNA and protein levels.

$Ly6C^{hi}$ Th Cells Promote Substantially Higher Plasma Cell Production In Vivo

To assess each naive Th cell subset's capacity for regulating B cell immunity, we developed an exclusion adoptive transfer model of specific humoral immunity. We have experience in the quantitative cellular analysis of the Th cell-regulated B cell response to the hapten (4-hydroxy-3-nitrophenyl)acetyl NP conjugated to the protein carrier keyhole limpet hemocyanin (KLH) (McHeyzer-Williams et al., 1991, 2000; Shapiro-Shelef et al., 2003). We can directly estimate the extent and quality of the B cell response to this antigen in C57BL/6 mice (same balance of $Ly6C^{hi}$ and $Ly6C^{lo}$ naive Th cell subsets as the B10.BR strain; data not shown). First, we transferred unfractioned spleen cells into Rag-1-deficient recipients, immunized immediately with NP-KLH in the Ribi adjuvant system, and evaluated the extent of the antigen-specific response and resultant subset balance 10–14 days later (Figure 2A). Using this approach, we promoted a robust NP-specific B cell response ($PI^-CD4^-CD8^-NP^+IgD^-$; 0.5 ± 0.2%) with a large NP-specific plasma cell compartment ($CD138^+B220^{+/-}$; 35 ± 10%) and a large NP-specific preplasma memory B cell compartment ($CD138^-B220^-$ [McHeyzer-Williams et al., 2000; Driver et al., 2001; Shapiro-Shelef et al., 2003]), but with a low but detectable NP-specific GC and post-GC memory B cell compartment ($CD138^-B220^+$). Hence, these Rag-1-deficient splenic microenvironments were capable of mounting all cellular facets of a Th cell-regulated antigen-specific B cell responses.

Next, we transferred spleen cells sorted to exclude all $CD4^+CD44^{hi}$ Th cells (gating levels as for Figure 1C) and either the $Ly6C^{lo}$ or $Ly6C^{hi}$ naive Th cells (as depicted in Figure 2B). Thus, each recipient received only naive Th cells of one Ly6C phenotype and all other cells in the unfractionated spleen. On day 10 after NP-KLH immunization, we quantified total $PI^-CD4^-CD8^-IgD^-CD138^+B220^{+/-}$ cells regardless of antigen specificity (Figure 2B, last panel), the subset balance of NP-specific B cells (Figure 2C, first panel), and the number of NP-specific IgG-secreting cells by ELISPOT analysis direct ex vivo (no in vitro stimulus) from the spleen and bone marrow (Figure 2C, second panel). Using each of these three indices, plasma cell production was 10- to 100-fold higher in the presence of the $Ly6C^{hi}$ Th cell subset, with the most dramatic differences seen in the bone marrow response. While there were differences in the frequencies of $B220^-CD138^-$ preplasma memory B cells and the $B220^+CD138^+$ compartment, they were broadly supported by both Th cell subsets. Thus, the $Ly6C^{hi}$ naive Th cells appear uniquely subspecialized to promote plasma cell production in vivo.

Equivalent Th Cell Clonal Expansion In Vitro and In Vivo

Next, we examined the intrinsic capacity of each Th cell subset to proliferate in vitro. We assess this capacity for clonal expansion using strong polyclonal stimuli in vitro (anti-CD3, anti-CD28 in the presence of IL-2). We used an assay with single-cell resolution (Bikah et al.,

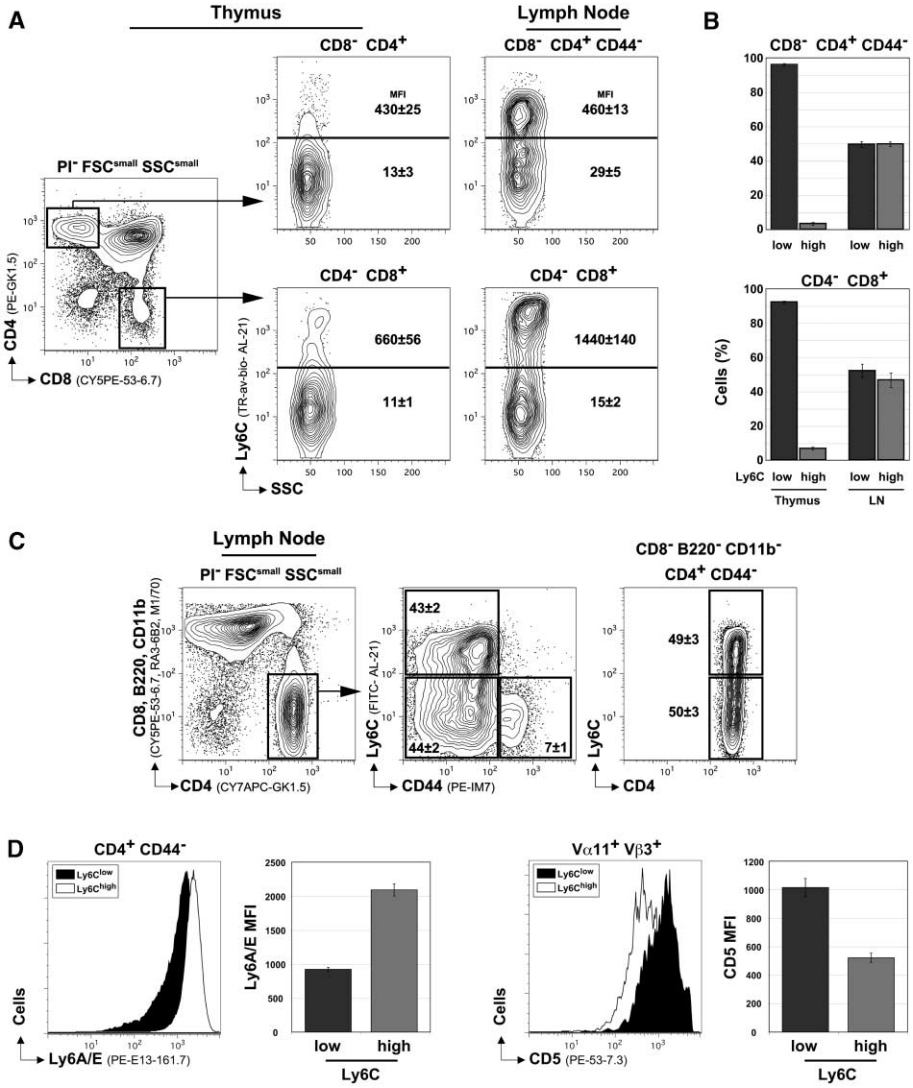

Figure 1. Ly6C Expression on Naive T Helper Cells Creates a Major Divide in the Periphery

(A) Representative probability contours of thymocytes (first two panels) and lymphocytes (third panel) from B10.BR mice. Ly6C levels on $PI^-CD8^-CD4^+$ cells (upper panels) and $PI^-CD4^-CD8^+$ cells (lower panels). Inserts are Ly6C mean fluorescence intensity ± SEM, n = 4.

(B) Frequency of Ly6C expression in the thymus and lymph node for $PI^-CD8^-CD4^+$ cells (upper panel) and $PI^-CD4^-CD8^+$ cells (lower panel). Mean ± SEM, n = 4.

(C) Representative probability contours of lymphocytes from B10.BR mice displayed as $PI^-CD8^-B220^-CD11b^-CD4^+$ (first and second panels) and $CD44^-$ and either $Ly6C^{hi}$ or $Ly6C^{lo}$ (third panel). Boxed inserts display frequencies of cells (mean ± SEM, n = 3).

(D) Ly6A/E expression (first panel), Ly6A/E MFI (second panel), CD5 expression (third panel), and CD5 MFI (fourth panel) on $CD4^+CD44^-$ naive Th cells with $Ly6C^{hi}$ or $Ly6C^{lo}$ phenotype; mean ± SEM, n = 3.

2000) that provides direct information on the frequency of responding Th cells and the extent of clonal expansion per responding clone (Figure 3A). A substantial fraction of individually sorted cells from both subsets responded to these stimuli (47 ± 9% and 45 ± 7% $Ly6C^{hi}$ and $Ly6C^{lo}$, respectively), and with a similar clonal burst size (an average of 32 ± 12 and 38 ± 7; n = 3 $Ly6C^{hi}$ and $Ly6C^{lo}$, respectively). Thus, both naive subsets of Th cells were equally capable of polyclonal expansion, regardless of their Ly6C phenotype.

We then devised an adoptive transfer system to assess each subset's capacity for antigen-driven clonal expansion in vivo. We took advantage of the elevated PCC-specific precursor frequency in 5C.C7β chain transgenic animals as previously demonstrated (Savage et al., 1999) (see tetramer binding profile in naive animals in Figure 6A). We sorted homogeneous populations of naive Th cells (Figure 3B; as $CD44^{lo}$ in this case, but these cells were also $CD62L^{hi}$) that were either $Ly6C^{hi}$ or $Ly6C^{lo}$ from these animals (see Ly6C profiles in Figure 6A) and transferred them intravenously into naive nonirradiated B10.BR hosts and immediately immunized subcutaneously with PCC in Ribi adjuvant. On the basis of our previous work (McHeyzer-Williams and Davis, 1995; McHeyzer-Williams et al., 1999), we quantified the $Vα11^+Vβ3^+$ Th cells (Figure 3C, first panel) responding to antigen using the modulation of cell surface molecules (upregulation of CD44 and downregulation of CD62L)

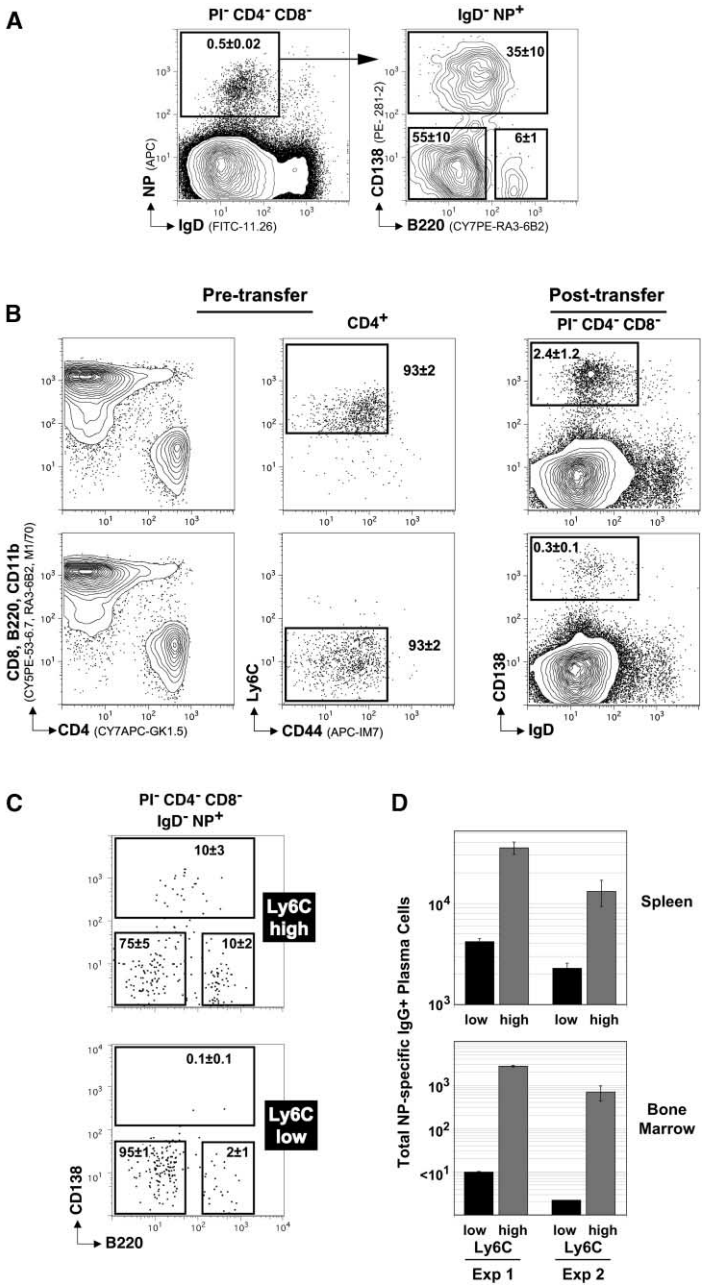

Figure 2. Ly6C^{hi} Th Cells Promote Plasma Cell Production In Vivo

(A) Unfractioned spleen cells from C57BL/6 mice transferred into Rag-1-deficient recipients, immunized with NP-KLH in Ribi, analyzed at day 14. Representative probability contours of PI$^-$CD4$^-$CD8$^-$ cells for NP and IgD (first panel). CD138 and B220 levels on NP-specific cells (second panel). Box inserts display mean frequencies ± SEM, n = 3.

(B) Exclusion cell transfers. The first two columns represent reanalysis of spleen and LN cells with sorted Ly6C^{hi} cells (excluding CD4$^+$Ly6C^{lo} and CD4$^+$CD44$^+$ cells) (top row) or Ly6C^{lo} cells (excluding CD4$^+$Ly6C^{hi} and CD4$^+$CD44$^+$ cells) (bottom row) for transfer into Rag-1-deficient recipients. Box inserts represent sort purity immediately prior to transfer; mean ± SEM, n = 3. Third column displays representative probability contours of splenic PI$^-$CD4$^-$CD8$^-$ cells 10 days after cell transfer and immunization with NP-KLH. CD138 and IgD levels are displayed for Ly6C^{hi} transfer (top) and Ly6C^{lo} transfer (bottom) transfers. Box insert highlights CD138$^+$IgD$^-$ total plasma cells (mean ± SEM, n = 3).

(C) CD138 and B220 profiles on PI$^-$CD4$^-$CD8$^-$NP$^+$IgD$^-$ spleen cells in Rag-1-deficient recipients 10 days after transfer and immunization. Upper panel from Ly6C^{hi} transfers and lower panel from Ly6C^{lo} transfers as described in (B). Box inserts display mean ± SEM, n = 3.

(D) NP-specific IgG Elispot analysis for total numbers of plasma cells in the spleen (upper panel) and bone marrow (lower panel) from animals 10 days after Ly6C^{hi} or Ly6C^{lo} transfers.

(Figure 3C, posttransfer, middle column), or the binding to pMHC II tetramers (Figure 3B, posttransfer, end column). There was an ~10-fold increase in the PCC-specific Th cell response 5 days after adoptive transfer (Figure 3D; Vα11Vβ3, Ly6C^{hi} compared to no transfer; p = 0.01). By day 10 after transfer, PCC-specific Th cell numbers were consistently lower using Ly6C^{lo} Th cells; however, there was no significant difference between the two populations (Figure 3D; Vα11Vβ3 p = 0.09; pMHC II$^+$ p = 0.1). Thus, both Th cell subsets clonally expanded to equivalent levels in response to antigen exposure with similar short-term survival in vivo.

Ly6C^{hi} Th Cell Subset Uniquely Supports Plasma Cell Development

While there was no difference in antigen-driven Th cell expansion, we wanted to confirm the impact of each naive Th cell subset on the antigen-driven B cell response in this more conventional adoptive transfer model using a different antigen and route of immunization. We can identify isotype-switched B cells (CD4$^-$ CD8$^-$ and IgM$^-$IgD$^-$) that are either plasma cells (CD138$^+$; Syndecan-1) or other B cells based on CD79b expression (Igβ BCR coreceptor and CD138$^-$) (Figure 4A). Plasma cell numbers were significantly lower at day 5 (p = 0.003) and day 10 (p = 0.03) after PCC immunization following Ly6C^{lo} compared to Ly6C^{hi} Th cell transfer (Figure 4B, CD138$^+$B220$^{+/-}$ displays plasma cell frequencies; Figure 4C, total numbers with comparisons to no transfer). The Ly6C^{lo} Th cells did not contribute to the early plasma cell response above the endogenous levels (Figure 4C, day 5 compared to no transfer). Once again, the capacity to support the early production of plasma cells uniquely assorted into the Ly6C^{hi} Th cell

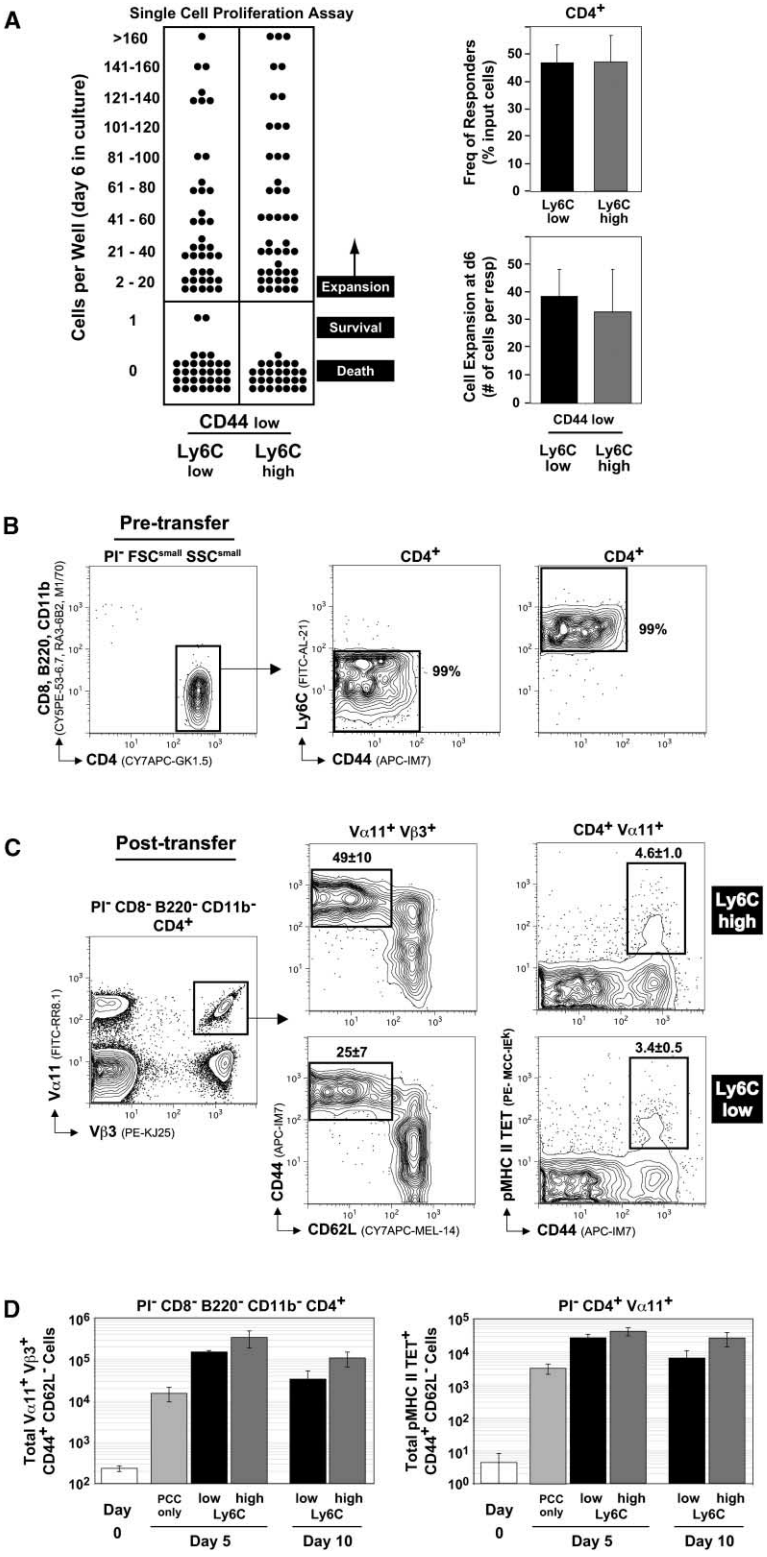

Figure 3. Similar Polyclonal and Antigen-Driven Expansion across Both Ly6C Th Cell Compartments

(A) Single PI$^-$CD8$^-$B220$^-$CD11b$^-$CD44^{lo} cells (left panel) that were Ly6C^{lo} (first column) or Ly6C^{hi} (second column) from B10.BR mice were sorted directly into 15 μl cultures containing IL2 with plate-bound anti-CD3, anti-CD28 (n = 72 cells for each population, n = 3 mice). PI$^-$CD8$^-$B220$^-$CD11b$^-$ cells contain >85% CD4$^+$ cells. Each filled circle represents the range of cells present in a separate well at day 6 in vitro (one representative experiment is shown). Frequency of responders (upper right panel) was calculated as the percentage of wells with ≥2 cells, mean ± SEM. Cell expansion at day 6 (lower right panel) was calculated as the average number of cells in wells with ≥2 cells for each population.

(B–D) Lymph node cells from 5C.C7β TCR transgenic mice with the desired phenotype were sorted and transferred into B10.BR mice. The B10.BR recipients were then immunized with 400 μg PCC in Ribi adjuvant.

(B) Representative probability contours of the purity of cells transferred. PI$^-$CD8$^-$B220$^-$CD11b$^-$CD4$^+$ cells (first panel) that were either CD44^{lo}Ly6C^{lo} (second panel) or CD44^{lo} Ly6C^{hi} (third panel). Box insert with the frequency of cells is shown.

(C) Representative probability contours of the B10.BR recipients for Vα11 and Vβ3 expression on PI$^-$CD8$^-$B220$^-$CD11b$^-$CD4$^+$ cells (first panel) responding to antigen using the modulation of CD44 and CD62L (second panel), or the binding to pMHC II tetramers (third column) 10 days after transfer of either Ly6C^{hi} (upper panels) or Ly6C^{lo} cells (lower panels). Boxed inserts, mean ± SEM, n = 3.

(D) Total number of Vα11Vβ3 expressing PI$^-$CD8$^-$B220$^-$CD11b$^-$CD4$^+$ cells that have upregulated CD44 and downregulated CD62L (left panel) or total number of pMHC II tetramer$^+$ PI$^-$CD4$^+$Vα11$^+$CD44$^+$CD62L$^-$ cells (right panel) for day 0 B10.BR mice with no immunization or cell transfer (first column), day 5 after PCC in Ribi adjuvant immunization and no cell transfer (second column), day 5 with immunization and Ly6C^{lo} cell transfer (third column), day 5 with immunization and Ly6C^{hi} cell transfer (fourth column), day 10 with immunization and Ly6C^{lo} cell transfer (fifth column), or day 10 with immunization and Ly6C^{hi} cell transfer (sixth column). Mean ± SEM, n = 3 for each condition.

compartment, consistent with the results in the splenic NP-specific B cell response.

Furthermore, both populations supported equivalent germinal center B cell responses (Figure 4B; CD79b$^+$ CD138$^-$B220$^+$ and GL7$^+$ frequencies, Figure 4D; total numbers for day 0 and 10). The preplasma memory B cell compartment was also equally supported by both Th cell subsets (Figure 4B, CD79b$^+$CD138$^-$B220$^-$ and GL7$^-$; Figure 4D, total cell numbers for day 0 and 10). These data are also consistent with the patterns demonstrated in the NP-specific B cell response. Both Ly6C Th cell subsets can support the more delayed B cell responses of germinal center formation and some aspects of memory B cell development. Hence, it appears

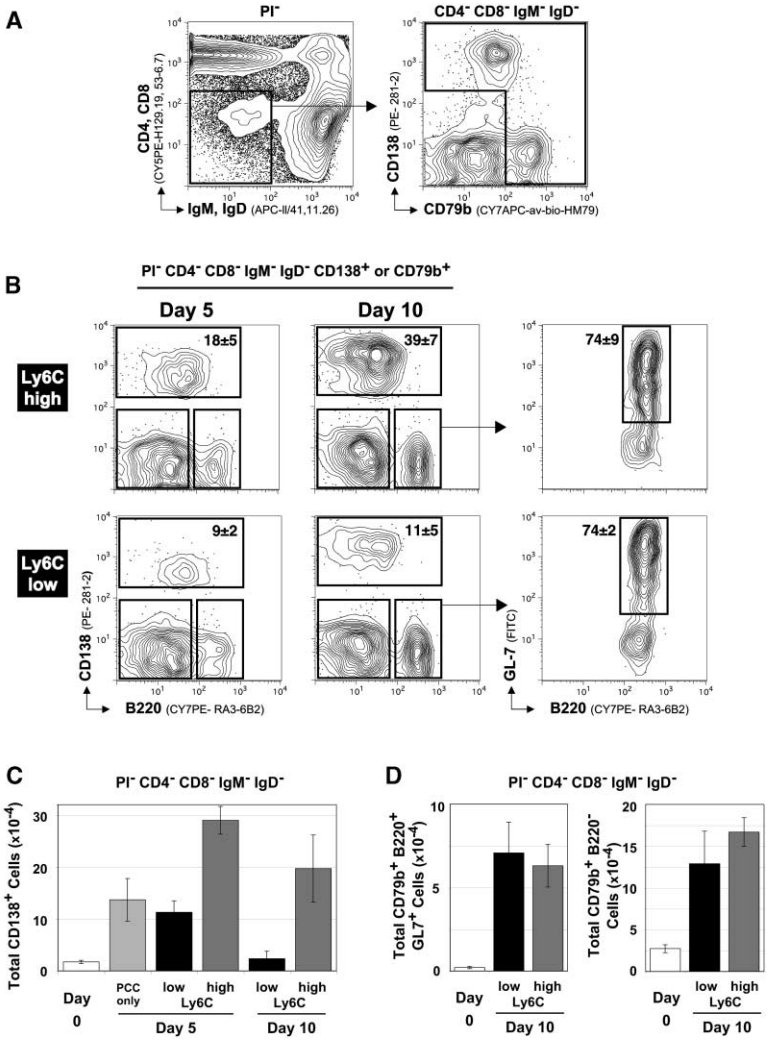

Figure 4. Ly6C^{hi} T Helper Cells Promote Plasma Cell Production

(A) As in Figure 3, lymph node cells from 5C.C7β TCR transgenic mice with the desired phenotype were transferred into B10.BR mice. The B10.BR hosts were then immunized with 400 μg PCC in Ribi adjuvant. Displayed are representative probability contours of the isotype-switched B cells at day 10. PI$^-$CD4$^-$CD8$^-$IgM$^-$IgD$^-$ cells (left plot) that express CD138 or CD79b (right plot).

(B) Representative probability contours of PI$^-$CD4$^-$CD8$^-$IgM$^-$IgD$^-$ CD138 or CD79b expressing cells at day 5 (first panel) or day 10 (second and third panels) post-cell transfer. GL7 levels for the isotype-switched B220$^+$ B cells (third panel). B10.BR mice that received 5C.C7β TCR transgenic Ly6C^{hi} (upper panels) or Ly6C^{lo} cells (lower panels) are displayed. Boxed inserts display the mean ± SEM, n = 3.

(C) Total number of isotype-switched (PI$^-$ CD4$^-$CD8$^-$IgM$^-$IgD$^-$) CD138 expressing B cells for days 0, 5, and 10 posttransfer into B10.BR mice (as described in Figure 3D). Mean ± SEM, n = 3 for each condition.

(D) Total number of isotype-switched (PI$^-$ CD4$^-$CD8$^-$IgM$^-$IgD$^-$) CD79b$^+$B220$^+$GL7$^+$ cells (left panel) and CD79b$^+$B220$^-$ cells (right panel) for days 0 and 10 post-Ly6C^{lo} or -Ly6C^{hi} cell transfer into B10.BR mice (as described in Figure 3D). Mean ± SEM, n = 3 for each condition.

that Ly6C^{hi} Th cells can support both the early and late phases of antigen-driven B cell differentiation while the Ly6C^{lo} only support the later phase of B cell differentiation.

Stable Upregulation of Ly6C in the Absence of Cell Division

In a final series of studies, we examine more closely the issues of development associated with this preexisting functional division in the naive Th cell compartment. First, we quantified the dynamics of peripheral Ly6C upregulation. We know that SP thymocytes are exported from the thymus expressing low levels of Ly6C (Figure 1A). We labeled whole thymocytes from B10.BR donors with CFSE and transferred them into nonirradiated B10.BR recipients (Figure 5A, first two panels). At various days after transfer, we focused analysis on either CD4 or CD8 SP Th cells with any CFSE label that reach the spleen or LNs (Figure 5A, second two panels). It is apparent from the two examples displayed (day 5 and 14 posttransfer) that Ly6C is upregulated in the absence of cell division as there is no difference in CFSE levels between Ly6C^{hi} and Ly6C^{lo} subsets. Thus, no selective expansion of a minor Th cell subset in the periphery can explain the appearance of the Ly6C^{hi} subset.

Three days after transfer, ~50% of the transferred CD4$^+$CD8$^-$ SP thymocytes in the spleens (or LNs displayed) of the donors upregulated Ly6C with no evidence of proliferation (Figure 5B). Ly6C distribution and level remained stable for at least 14 days (Figure 5B) with a low level of proliferation evident in both populations at this later time point (equivalent in both Ly6C compartments). In contrast, the Ly6C expression in CD8$^+$CD4$^-$ SP cells remained unchanged over this same period (Figure 5C) and is consistent with a need for overt T cell activation to induce Ly6C expression in the CD8 T cell compartment (Walunas et al., 1995; Tough et al., 1996). Therefore, unlike CD8$^+$ T cells, Ly6C is upregulated on half of all CD4$^+$ SP thymocytes within 3 days of exit from the thymus as a relatively stable phenotypic change without evidence of clonal expansion.

Upregulation of Ly6C Is Predetermined in the Thymus

To ascertain whether Ly6C upregulation in the periphery was a consequence of a secondary peripheral selection event based on TCR specificity, we excluded MHC ex-

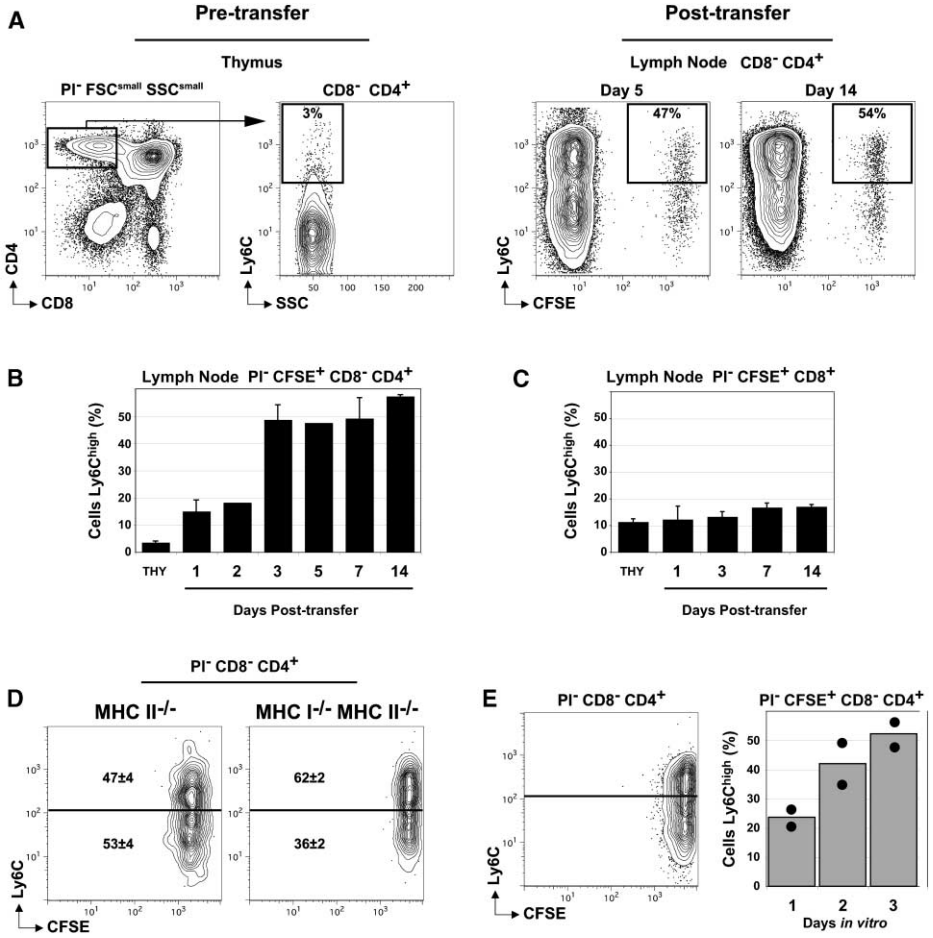

Figure 5. Ly6C^{hi} Cells Emerge in the Periphery without Cell Division and in the Absence of pMHC

(A) Representative probability contours of B10.BR thymus labeled with CFSE and transferred into nonirradiated B10.BR recipients (first two panels). Ly6C and CFSE levels on PI$^-$CD8$^-$CD4$^+$ lymphocytes 5 days (third panel) and 14 days (last panel) after transfer.

(B) The frequency of Ly6C^{hi} thymocyte donor cells (first column) and the frequency of Ly6C expression in the lymph node for PI$^-$ CFSE$^+$CD8$^-$CD4$^+$ cells. The days after transfer are indicated with mean ± SEM displayed. Except days 2 and 5 (n =1), each time point represents three mice.

(C) The frequency of Ly6C^{hi} thymocyte donor cells (first column) and the frequency of Ly6C expression in the lymph node for PI$^-$ CFSE$^+$CD4$^-$CD8$^+$ cells. The days after transfer are indicated with mean ± SEM, n = 3 displayed.

(D) Representative probability contours of CFSE-labeled C57BL/6 thymus after transfer into MHC class II-deficient mice (left plot) and MHC class I and class II double-deficient mice (right plot). Ly6C and CFSE levels on PI$^-$CD8$^-$CD4$^+$ lymphocytes 3 days after transfer with mean ± SEM, n = 3 displayed.

(E) CFSE-labeled thymocytes from B10.BR mice incubated in microculture medium. Cells were harvested, and a representative probability contour plot is displayed for day 3 (left plot) with the frequency of PI$^-$CFSE$^+$CD8$^-$CD4$^+$Ly6C^{hi} for various days shown (right graph). n = 2, with circles indicating individual experiments.

pression from the peripheral compartment. We repeated the CFSE thymus label and transfer experiments from C57BL/6 (same Ly6C distribution in the thymus and periphery; data not shown) into animals deficient in either MHC II alone or MHC I and MHC II double-deficient animals. By day 3 after transfer, ~50% of the CD4 SP thymocytes had upregulated Ly6C (Figure 5D). While these data do not exclude cytokine involvement in the periphery, TCR engagement was not involved in the upregulation of Ly6C by naive CD4 Th cells.

Finally, to indicate whether some other signal from the periphery was required for this differentiation event, we simply dissociated B10.BR thymocytes into microculture medium and assayed for Ly6C expression on the surviving SP thymocytes (Figure 5E). After 3 days in vitro and with no influence of the peripheral environment, ~50% of CD4 SP thymocytes upregulated Ly6C expression. Taken together with the previous transfer studies, these data suggest that Ly6C upregulation in a major fraction of naive Th cells in the periphery is a predetermined developmental consequence of events that occurred during thymic maturation.

Clonal Assortment within an Antigen-Specific Th Cell Compartment

To address the impact of thymic selection on the Ly6C cell fate decision, we chose to analyze TCR repertoire distribution. We reasoned that a preexisting divide in Th

cell precursors would assort all TCR specificities evenly into Ly6C^{hi} and Ly6C^{lo} compartments. In contrast, if thymic selection influenced the peripheral Ly6C decision then TCR specificities would assort unevenly into these two compartments. To distinguish between these two hypotheses, we used 5C.C7β chain transgenic animals that have a fixed TCRβ chain but polyclonal TCRα. We focused cellular and repertoire analysis on Th cells that expressed Vα11 V regions paired with the 5C.C7 TCRβ chain (Figure 6). Low levels of Ly6C in the thymus and an even distribution of Ly6C^{hi} and Ly6C^{lo} in the periphery were similar to that seen in nontransgenic B10.BR for this Vα11$^+$Vβ3$^+$ subset (data not shown).

Using pMHC II tetramers, we next directly isolated PCC-specific Th cells from the preimmune repertoire of the 5C.C7β chain transgenic animals (Figure 6A, first panels). Ly6C distribution within this naive antigen-specific compartment parallels that seen in the total CD4 population (Figure 6A, second panels). Individual cells from each of the cellular compartments were sorted for repertoire studies focused on Vα11CDR3 diversity (Figure 6B; RT-PCR efficiency 84 ± 3% of single cells). As expected, Jα usage for this Vα11$^+$ pMHC II$^+$ compartment in the thymus was more restricted than the total Vα11$^+$ cells (data not shown; 11 different Jα used; Jα13 and Jα22 at highest prevalence). The two peripheral Ly6C compartments were broadly different from the Ly6C^{lo} cells in the thymus and substantially different from each other (data not shown; $p = 0.015$; chi-square test comparing Jα with representatives in each subset).

Full peptide sequence analysis for the naive PCC-specific compartment in the periphery provides the strongest evidence for repertoire assortment at the level of TCR clonotype (Figure 6B). Many specific clonotypes with multiple representatives assort either Ly6C^{hi} or Ly6C^{lo} (Figure 6B, top two panels). A smaller number of clonotypes assort into both peripheral subsets (Figure 6B, bottom panel). However, only a few of these clonotypes assort evenly across both subsets (e.g., Jα22 with A at α94; this Jα22A assorts seven and six clones into each subset) with many others still markedly skewed (Jα13A skewing 8:1, Jα22S skewing 7:1, and Jα34A skewing 1:5 Ly6C^{hi} versus Ly6C^{lo}, respectively). Therefore, in the peripheral TCR repertoire, clones that are specific for a single foreign pMHC II complex are divided asymmetrically across the two phenotypically distinct naive peripheral Th subsets.

Ly6C Upregulation in the Periphery Is a Consequence of Thymic Selection

We next used TCRαβ transgenic animals to examine the impact of thymic selection on the peripheral Ly6C phenotype. The distribution of Ly6C on CD4$^+$CD8$^-$ SP thymocytes from three different PCC-specific transgenic mice was uniformly low (Figures 6C, left panels, and 6D, summary across multiple animals). The 5C.C7 and AND TCR are very similar structurally. Both transgenic animals preferentially assort Th cells into the Ly6C^{hi} compartment in the periphery when selected in the I-E^k thymic environment (Figures 6C and 6D, lower panels; 78 ± 1% and 82 ± 5% Ly6C^{hi}, respectively). This skewing was dramatically reversed for the AND TCR selected on I-A^b background as the vast majority of the peripheral Th cells remained Ly6C^{lo} (Figures 6C and 6D, 98 ± 0.5%). Thus, expression of a monoclonal TCR and the nature of the thymic selecting environment substantially influenced the peripheral Ly6C decision. More importantly, the identical TCR assorted differentially when placed in different selecting environments.

Discussion

Our studies identify a preexisting level of organization to the preimmune Th cell compartment. Differential Ly6C expression by naive Th cells in the periphery indicates alternate developmental fates established during thymic maturation. This phenotypic distinction occurs 3 days after thymic export and does not require cell division or engagement of the TCR in the periphery. In contrast, TCR expression and specificity in the thymus play an important role determining the peripheral Ly6C cell fate decision. This central selection event unevenly assorts the preimmune TCR repertoire, such that different clonotypes of Th cells specific for the same foreign pMHC II complex separate across the two peripheral Th cell subsets. Functionally, the Ly6C^{hi} subset appears uniquely able to support early plasma cell development in vivo, a critical and necessary function for effective humoral immunity.

A Major Division in Preimmune Th Cell Phenotype

Differential Ly6C expression has been well described (Rock et al., 1989), but the origins and impact of this phenotype in Th cells is not understood. Ly6C can enhance TCR signal transduction (Lee et al., 1994) and costimulate T cell responsiveness (Malek et al., 1986). Its GPI-anchored localization to lipid rafts (Bohuslav et al., 1993) provides some indication of a direct role in early T cell activation; however, this has not been demonstrated for Th cells in vivo. Preliminary studies indicate that Ly6C is lost very early in vivo on antigen-activated Th cells (by day 3 after PCC-specific activation in vivo; L.J.M.-W., unpublished data) and remains low thereafter. While many CD44^{hi} CD8$^+$ T cells express very high levels of Ly6C (Walunas et al., 1995; Tough et al., 1996) (data not shown), all CD44^{hi}CD4$^+$ Th cells express the lower level of Ly6C seen in the periphery (see Figure 1C). These trends are consistent with a proposed role for Ly6C in the early modulation of TCR-mediated signal transduction in vivo.

A Peripheral Consequence of Thymic Maturation

Ly6C itself is not playing a role in the thymic developmental decision that creates the peripheral cellular division. Differential expression of Ly6C in the periphery is a consequence of central selection events that impact developmental programming. The thymic adoptive transfer and in vitro experiments strongly support this notion (Figure 5). The time delay in Ly6C upregulation without cell division excludes peripheral clonal expansion and indicates a major developmental divide at the level of thymic maturation. The short-term stability of this phenotypic balance in the absence of cell division (to day 14, Figure 5) further supports the argument for a developmental divide that originates in the thymus and not as a response to peripheral stimuli (Goldrath

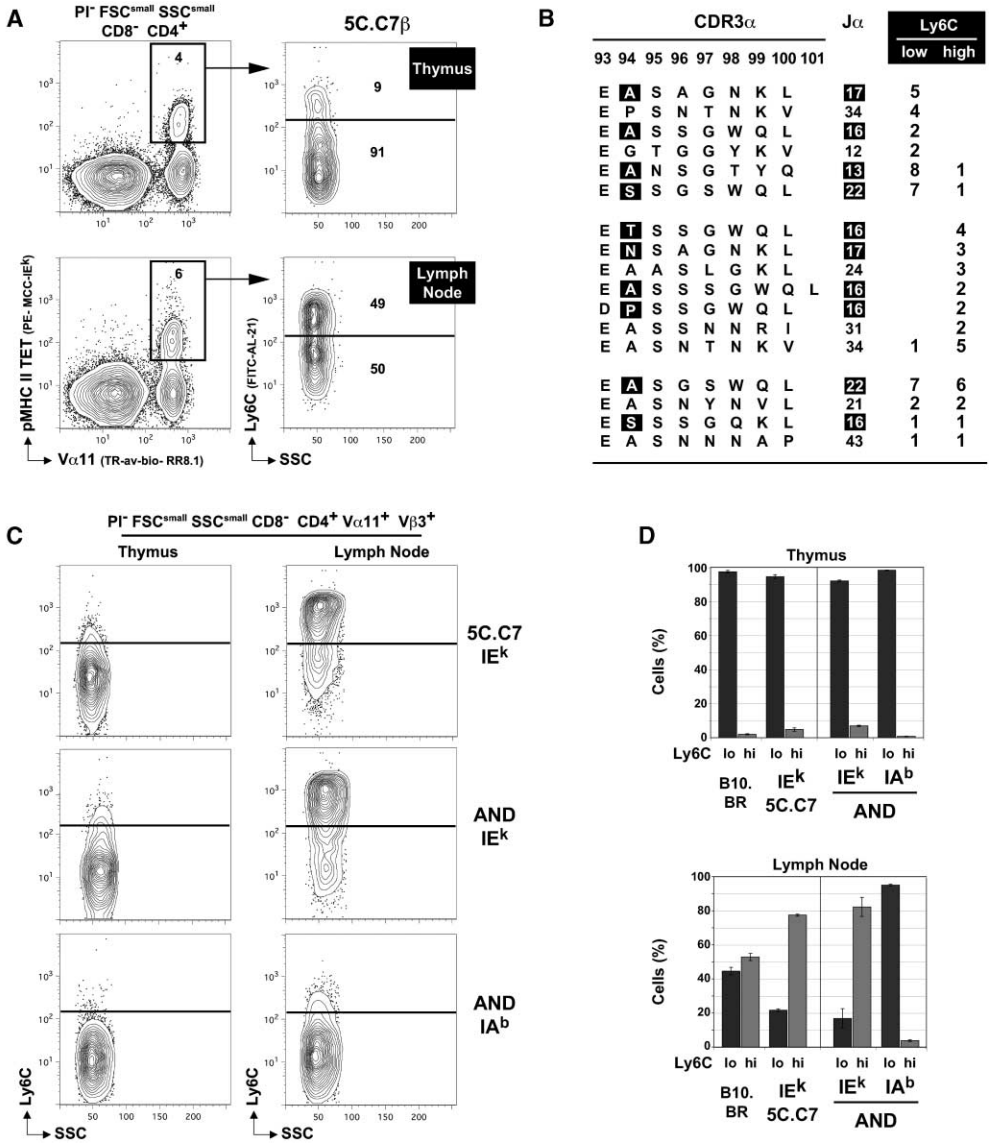

Figure 6. Clonal Assortment within an Antigen-Specific Th Cell Compartment

(A) Representative probability contours for thymocytes (upper panels) and lymphocytes (lower panel) from 5C.C7β TCR-transgenic mice. Vα11 and pMHC II tetramer levels (left panels) on PI$^-$CD8$^-$CD4$^+$ cells and Ly6C expression on PI$^-$CD8$^-$CD4$^+$Vα11$^+$ pMHC II TET$^+$ cells (right panels). Boxed inserts with the frequency are displayed.

(B) The TCR Vα11 amino acid sequence for the CDR3 region of single cells from lymph nodes of 5C.C7β TCR transgenic mice. Individual PI$^-$CD8$^-$CD4$^+$Vα11$^+$ pMHC II TET$^+$ clonotypes are displayed. The CDR3α region (aa 93 to 102), Jα usage, and number of cells with each clonotype and their distribution across the peripheral Ly6C^{lo} and Ly6C^{hi} compartments. A total of 98 cells were sequenced. Clonotypes that appeared once were excluded from the display.

(C) Ly6C expression on PI$^-$CD8$^-$CD4$^+$Vα11$^+$Vβ3$^+$ thymocytes (left panels) and lymphocytes (right panels) from 5C.C7αβ (top row), AND IE^k background (middle row), and AND IA^b background (bottom row) TCR transgenic mice.

(D) Frequency of Ly6C expression in the thymus (upper panel) and lymph node (lower panel) for PI$^-$CD8$^-$CD4$^+$Vα11$^+$Vβ3$^+$ cells from B10.BR mice and 5C.C7αβ, AND IE^k, and AND IA^b TCR transgenic mice. Mean ± SEM, n = 3.

and Bevan, 1999). However, these experiments do not indicate which stage of thymic maturation must be reached before the peripheral Ly6C decision has been imprinted. SP thymocytes reside in the thymic medulla for up to 2 weeks before export into the periphery (Scollay and Godfrey, 1995). Hence, all CD4 SP thymocytes may not be capable of the peripheral phenotypic change.

The majority of CD4 SP thymocytes (69 ± 2%; n = 3) express high levels of CD69 (Rosen et al., 2003) that needs to be lost before they exit to the periphery. We have recently uncovered a CD69 intermediate CD4 SP subset (19 ± 1%; n = 3) in this process that appears to be regulated independently of its CD69 predecessor and is developmentally upstream from the CD69 negative CD4 SP thymocyte (4 ± 0.2%; n = 3) (Rosen et al., 2003). It is this latter population that cross the thymic endothelial barrier into the blood. Thus, the precise cel-

lular checkpoints associated with the Ly6C developmental decision in the thymus are yet to be resolved.

Asymmetric Clonal Assortment in the Preimmune Th Cell Compartment

Regardless of when the Ly6C decision is fully imprinted in the thymus, it appears to rely on TCR and self-pMHC II expression in the thymus (Figures 5 and 6). Transgenic animals with fixed TCRβ chains are invaluable tools for the analysis of restricted but polyclonal preimmune repertoires. The increased resolution of specific pMHC II binding in the thymus and periphery allowed us to quantify directly the uneven assortment of antigen-specific clones across the two peripheral Th cell subsets (Figures 6A and 6B). Recent studies directly estimate tetramer binding half-lives of pMHC II$^+$ T cells in the 5C.C7β chain model (Savage and Davis, 2001). When comparing the sequence in each peripheral Ly6C compartment (Figure 6B) to the consensus sequence for TCR estimated to have slow half-lives (Savage and Davis, 2001), we saw no correlation across the two peripheral subsets, suggesting that different TCR half-lives were not the driving mechanism for assortment.

Using TCR$\alpha\beta$ transgenic animals (Figures 6C and 6D), we further implicate TCR-self-pMHC II specificity. Distribution of CD5 levels as an indicator of signal strength in the thymus (Azzam et al., 2001) across the different TCR$\alpha\beta$ transgenic animals (data not shown), argues against a model in which the overall "strength of the signal" determines peripheral Ly6C fate. Nevertheless, clonal assortment appears to be driven by TCR specificity against a spectrum of self-pMHC II complexes in the thymus, but the directing quality of this signal remains elusive.

A Preimmune Division in Th Cell Functional Potential

The asymmetric assortment of peptide-specific TCR repertoires underscores the intriguing possibility of a preexisting functional divide in naive Th cells. The capacity of both subsets for substantial and equivalent polyclonal (Figure 3A) and antigen-driven (Figures 3B and 3C) expansion argued against a suppressor/inducer functional divide (Sakaguchi et al., 1995). Screens for differential CD25 levels (data not shown) further argued against this possibility. On the other hand, quantifying the developing B cell response to protein antigen immunization amplifies a most relevant effector Th cell activity in vivo (Figures 2 and 4). Both naive Th cell subsets provide help to B cells in these immune responses by promoting germinal centers and the formation of preplasma memory B cells (Figures 2B, 2C, 4B, and 4D) (McHeyzer-Williams et al., 2000; Driver et al., 2001; Shapiro-Shelef et al., 2003). While we have not yet directly tested a Th1/Th2 functional divide in the antigen-specific Th cell subsets, this B cell helper capacity suggests both populations can produce a Th2 response. These functional distinctions may be more reminiscent of the B helper versus inflammatory CD4 Th subset divide proposed by Butcher and colleagues (Campbell et al., 2001); however, these distinctions were thought to be derived and not preexisting.

The fundamental functional difference found in these initial studies was the unique capacity of the Ly6C^{hi} Th cell subset to promote robust early plasma cell development (Figures 2 and 4). The same pattern was established across two separate adoptive transfer systems using different antigens and route of immunization. Many gene ablation models, CD40/CD40L being the best-characterized example (Armitage et al., 1992), result in a block in germinal center development but leave the antibody-secreting pathway intact (McHeyzer-Williams and Ahmed, 1999). This is also true for ablation of ICOS and ICOSL, a more recently described member of the B7/CD28 family of molecules (Mak et al., 2003). Ablation of the *SAP* gene (Crotty et al., 2003) provides another recent example of a CD4 defect in which B cell isotype switch and early plasma cell production is left intact, but germinal center formation and postgerminal center activities are lost. While these studies point to defects or deviations in normal Th cell responsiveness, they are also consistent with the loss of preexistence of functionally distinct Th cell compartments.

The existence of a more rudimentary regulatory mechanism for the production of germline-encoded antibody to thymus-dependent antigens would provide substantial survival advantage over a totally T cell-independent immune system. Thus, the Ly6C^{hi} Th cell subset may also be a phylogenetically more distant layer of cellular regulation in the mammalian adaptive immune system.

Concluding Remarks

One overriding strategy for the immune system is the utility of cellular subspecialization. Many aspects of diverse lymphocyte function are preprogrammed during development and layered into the preimmune compartment. Self-antigens are used to eliminate self-reactivity, but they also shape the final immune-responsive repertoire. Our current studies identify a major developmental division in the preimmune Th cell compartment that is recognizable through the differential expression of Ly6C. Our initial functional studies identify a prominent role for the Ly6C^{hi} naive Th cells in the regulation of plasma cell development in vivo; however, the full impact of this cellular divide on the development of effective and protective humoral immunity remains to be determined.

Experimental Procedures

Mice

B10.BR, C57BL/6 mice, and Rag-1-deficient mice were bred at The Scripps Research Institute or purchased from the Jackson Laboratory (Bar Harbor, ME). The 5C.C7$\alpha\beta$ TCR Tg, 5C.C7β TCR Tg (Jorgensen et al., 1992) mice were obtained from Mark Davis (Stanford University, CA), AND TCR Tg on a C57BL/6 background from Carolyn Doyle (Duke University, NC), AND TCR Tg on a B10.BR background from Susan Swain (Trudeau Institute, NY) (Haynes et al., 1999), MHC class II-deficient and MHC class I and class II double-deficient mice (Grusby et al., 1991, 1993) from Carolyn Doyle. All mice were maintained under specific pathogen-free conditions at Duke University or The Scripps Research Institute.

Flow Cytometry

The thymus, spleen, and lymph nodes were harvested as previously described (McHeyzer-Williams et al., 1999). Cells were stained at 2×10^8 cells/ml on ice for 45 min. PE-MCC-IE^k tetramer staining was done at room temperature for 45 min. The following antibodies were used for labeling cells and conjugated in the McHeyzer-Williams laboratory: FITC-RR8.1 (α-Vα11), PE-GK1.5 (α-CD4), PE-KJ25

(α-Vβ3), APC-KJ25 (α-Vβ3), APC-IM7 (α-CD44), NP-APC, APC-11.26 (α-IgD; a gift from F. Finkelman, University of Cincinnati Medical Center, OH), Texas Red-KJ25 (α-Vβ3), Texas Red-IM7 (α-CD44), biotin-RR8.1 (α-Vα11), biotin-HM79b (α-Igβ/CD79b), and PE-MCC-IE^k (pMHC II tetramer; a gift from Mark Davis, Stanford University, CA), The following were purchased: from BD Pharmingen, FITC-AL-21 (α-Ly6C), FITC-GL7, PE-53-7.3 (α-CD5), PE-E13-16.17 (α-Ly6A/E), PE-281-2 (α-CD138), Cy5PE-53-6.7 (α-CD8), Cy5PE-RA3-6B2 (α-B220), Cy5PE-H129.19 (α-CD4), APC-II/41 (α-IgM), biotin-AL-21 (α-Ly6C); from Caltag, Cy5PE-M1/70.15 (α-CD11b), Cy7PE- RM4-5 (α-CD4), Cy7PE-RA3-6B2 (α-B220); and from eBiosciences, Cy5PE-MEL-14 (α-CD62L), Cy7APC-MEL-14 (α-CD62L). Streptavidin-Texas Red or streptavidin-Cy7APC (BD Pharmingen) was used as a second-step revealing reagent.

Cells were washed twice in PBS with 5% FCS and resuspended in 2 mg/ml propidium iodide (PI) with 5% FCS. Samples were analyzed using Cell Quest software on a FACSVantage SE (BD Pharmingen). Standard analog compensation was used with Ominicomp correction between Cy5PE, Cy7PE, and APC, Cy7APC. Data were analyzed using FlowJo software (Tree Star). Profiles are presented as 5% probability contours with outliers.

Adoptive Transfer and Thymic Cultures

Unfractionated spleen cells (2.5–5 × 10^7) from C57BL/6 mice were transferred into Rag-1-deficient mice. Exclusion adoptive transfers used 5.5–25 × 10^6 spleen and LN cells combined and sorted as described (Figure 2), and transferred IV (n = 2) and immunoprecipitated (n = 2) into Rag-1-deficient recipients. Purity of sorted populations was reanalyzed immediately before transfer. Recipients were immunized IP with 400 μg NP-KLH in the Ribi adjuvant system (Corixa) 4–12 hr after transfer. Spleens and bone marrow were harvested from the recipient mice 10–12 days after immunization and processed as described above. Enzyme-linked immunospot (ELISPOT) for detection of NP-specific IgG was performed as described previously (McHeyzer-Williams et al., 2000). 0.9–1.2 × 10^6 5C.C7β lymph node cells with the desired phenotype were sorted and transferred intravenously into B10.BR mice. The B10.BR mice were immediately immunized base of tail with 400 μg PCC (pigeon cytochrome c, Sigma) in Ribi adjuvant. Freshly harvested thymocytes were labeled with 5 μM CFSE (carboxy-fluorescein succinimidyl ester, Molecular Probes) for 5 min at 27°C and washed three times. 5–14 × 10^7 CFSE-labeled thymocytes were transferred IP. For thymic in vitro cultures, 5 × 10^5 thymocytes/well-labeled with 5 μM CFSE in microculture medium (DMEM, 10% FCS, 1 U/ml penicillin and streptomycin, 2 mM L-glutamine, 50 μM 2-mercaptoethanol) were incubated at 37°C and 10% CO_2.

Single-Cell Proliferation Assay

Single-cell proliferation studies were performed as previously described (Bikah et al., 2000). In brief, single T cells with the appropriate phenotype were sorted directly into 72-well trays (Robbins Scientific) precoated with α-CD3 (20 μg/ml) and α-CD28 (10 μg/ml) in the presence of 10 U/ml IL-2 (PeproTech), in 15 μl of microculture medium (1640 RPMI, 10% FCS, 1 U/ml penicillin and streptomycin, 2 mM L-glutamine, 50 μM 2-mercaptoethanol) and incubated for 6 days at 37°C and 5% CO_2. The presence of cells was scored using phase contrast microscopy by a person "blinded" to the culture conditions and phenotype of the cells.

Single-Cell Repertoire Analysis

Single-cell repertoire studies were performed as previously described (McHeyzer-Williams et al., 1999). In brief, single T cells with the appropriate surface phenotype were sorted into oligo d(T) primed 5 μl cDNA reactions, held at 37°C for 90 min, and then stored at −80°C until further use. Two microliters of cDNA reaction was used in a 25 μl Vα11-specific 40 cycle PCR reaction, and then 1 μl of this first PCR reaction was used for a second Vα11-specific 35 cycle PCR reaction using primers nested medially to the first set. First round primers: sense, 5′-AATCTGCAGTGGGTGCAGATTTGC TGG-3′; antisense, 5′-AATCTGCAGCGGCACATTGATTTGGGA-3′. Second round primers: sense, 5′-AGATTTGCTGGGTGAGAGGAG-3′; antisense, 5′-GAGTCAAAGTCGGTGAACAGG-3′. One negative control (no cell sorted into the cDNA reaction) every five samples were processed simultaneously to control for contamination. Second PCR reaction was screened for positives, column separated from the primers and directly sequenced using an ABI 373 automated sequencing system. The frequency for obtaining a sequenceable PCR product from single cells was 57 ± 5 for Vα11$^+$Vβ3$^+$ cells and 84 ± 3 for Vα11$^+$Tet$^+$ cells.

Acknowledgments

We would like to thank Jessica Ebright and Adam O'Connor for expert technical assistance and Linda Sherman and Laurent Malherbe for critical appraisal of the manuscript. This work was supported by NIH grants AI40215 and AI47231.

Received: August 11, 2003
Revised: January 19, 2004
Accepted: January 27, 2004
Published: February 17, 2004

References

Apostolopoulos, J., McKenzie, I.F., and Sandrin, M.S. (2000). Ly6d-L, a cell surface ligand for mouse Ly6d. Immunity *12*, 223–232.

Armitage, R.J., Fanslow, W.C., Strockbine, L., Sato, T.A., Clifford, K.N., Macduff, B.M., Anderson, D.M., Gimpel, S.D., Davis-Smith, T., Maliszewski, C.R., et al. (1992). Molecular and biological characterization of a murine ligand for CD40. Nature *357*, 80–82.

Azzam, H.S., DeJarnette, J.B., Huang, K., Emmons, R., Park, C.S., Sommers, C.L., El-Khoury, D., Shores, E.W., and Love, P.E. (2001). Fine tuning of TCR signaling by CD5. J. Immunol. *166*, 5464–5472.

Bamezai, A., and Rock, K.L. (1995). Overexpressed Ly-6A.2 mediates cell-cell adhesion by binding a ligand expressed on lymphoid cells. Proc. Natl. Acad. Sci. USA *92*, 4294–4298.

Bikah, G., Pogue-Caley, R.R., McHeyzer-Williams, L.J., and McHeyzer-Williams, M.G. (2000). Regulating T helper cell immunity through antigen responsiveness and calcium entry. Nat. Immunol. *1*, 402–412.

Bohuslav, J., Cinek, T., and Horejsi, V. (1993). Large, detergent-resistant complexes containing murine antigens Thy-1 and Ly-6 and protein tyrosine kinase p56lck. Eur. J. Immunol. *23*, 825–831.

Campbell, D.J., Kim, C.H., and Butcher, E.C. (2001). Separable effector T cell populations specialized for B cell help or tissue inflammation. Nat. Immunol. *2*, 876–881.

Crotty, S., Kersh, E.N., Cannons, J., Schwartzberg, P.L., and Ahmed, R. (2003). SAP is required for generating long-term humoral immunity. Nature *421*, 282–287.

Driver, D.J., McHeyzer-Williams, L.J., Cool, M., Stetson, D.B., and McHeyzer-Williams, M.G. (2001). Development and maintenance of a B220- memory B cell compartment. J. Immunol. *167*, 1393–1405.

Goldrath, A.W., and Bevan, M.J. (1999). Selecting and maintaining a diverse T-cell repertoire. Nature *402*, 255–262.

Grusby, M.J., Johnson, R.S., Papaioannou, V.E., and Glimcher, L.H. (1991). Depletion of CD4+ T cells in major histocompatibility complex class II-deficient mice. Science *253*, 1417–1420.

Grusby, M.J., Auchincloss, H., Jr., Lee, R., Johnson, R.S., Spencer, J.P., Zijlstra, M., Jaenisch, R., Papaioannou, V.E., and Glimcher, L.H. (1993). Mice lacking major histocompatibility complex class I and class II molecules. Proc. Natl. Acad. Sci. USA *90*, 3913–3917.

Haynes, L., Linton, P.J., Eaton, S.M., Tonkonogy, S.L., and Swain, S.L. (1999). Interleukin *2*, but not other common gamma chain-binding cytokines, can reverse the defect in generation of CD4 effector T cells from naive T cells of aged mice. J. Exp. Med. *190*, 1013–1024.

Jacob, J., Kelsoe, G., Rajewsky, K., and Weiss, U. (1991). Intraclonal generation of antibody mutants in germinal centres. Nature *354*, 389–392.

Jorgensen, J.L., Esser, U., Fazekas de St Groth, B., Reay, P.A., and Davis, M.M. (1992). Mapping T-cell receptor-peptide contacts by variant peptide immunization of single-chain transgenics. Nature *355*, 224–230.

Lee, S.K., Su, B., Maher, S.E., and Bothwell, A.L. (1994). Ly-6A is

required for T cell receptor expression and protein tyrosine kinase fyn activity. EMBO J. *13*, 2167–2176.

Mak, T.W., Shahinian, A., Yoshinaga, S.K., Wakeham, A., Boucher, L.M., Pintilie, M., Duncan, G., Gajewska, B.U., Gronski, M., Eriksson, U., et al. (2003). Costimulation through the inducible costimulator ligand is essential for both T helper and B cell functions in T cell-dependent B cell responses. Nat. Immunol. *4*, 765–772.

Malek, T.R., Ortega, G., Chan, C., Kroczek, R.A., and Shevach, E.M. (1986). Role of Ly-6 in lymphocyte activation. II. Induction of T cell activation by monoclonal anti-Ly-6 antibodies. J. Exp. Med. *164*, 709–722.

McHeyzer-Williams, M.G. (2003). B cells as effectors. Curr. Opin. Immunol. *15*, 354–361.

McHeyzer-Williams, M.G., and Davis, M.M. (1995). Antigen-specific development of primary and memory T cells in vivo. Science *268*, 106–111.

McHeyzer-Williams, M.G., and Ahmed, R. (1999). B cell memory and the long-lived plasma cell. Curr. Opin. Immunol. *11*, 172–179.

McHeyzer-Williams, M.G., Nossal, G.J.V., and Lalor, P.A. (1991). Molecular characterization of single memory B cells. Nature *350*, 502–505.

McHeyzer-Williams, M.G., McLean, M.J., Lalor, P.A., and Nossal, G.J.V. (1993). Antigen-driven B cell differentiation in vivo. J. Exp. Med. *178*, 295–307.

McHeyzer-Williams, L.J., Panus, J.F., Mikszta, J.A., and McHeyzer-Williams, M.G. (1999). Evolution of antigen-specific T cell receptors in vivo: preimmune and antigen-driven selection of preferred complementarity-determining region 3 (CDR3) motifs. J. Exp. Med. *189*, 1823–1838.

McHeyzer-Williams, L.J., Cool, M., and McHeyzer-Williams, M.G. (2000). Antigen-specific B cell memory: expression and replenishment of a novel B220- memory B cell compartment. J. Exp. Med. *191*, 1149–1166.

Panus, J.F., McHeyzer-Williams, L.J., and McHeyzer-Williams, M.G. (2000). Antigen-specific T helper cell function: differential cytokine expression in primary and memory responses. J. Exp. Med. *192*, 1301–1316.

Pflugh, D.L., Maher, S.E., and Bothwell, A.L. (2002). Ly-6 superfamily members Ly-6A/E, Ly-6C, and Ly-6I recognize two potential ligands expressed by B lymphocytes. J. Immunol. *169*, 5130–5136.

Rock, K.L., Reiser, H., Bamezai, A., McGrew, J., and Benacerraf, B. (1989). The LY-6 locus: a multigene family encoding phosphatidylinositol-anchored membrane proteins concerned with T-cell activation. Immunol. Rev. *111*, 195–224.

Rosen, H., Alfonso, C., Surh, C.D., and McHeyzer-Williams, M.G. (2003). Rapid induction of medullary thymocyte phenotypic maturation and inhibition of thymic egress at low nanomolar concentrations of S1P receptor agonist. Proc. Natl. Acad. Sci. USA *100*, 10907–10912.

Sakaguchi, S., Sakaguchi, N., Asano, M., Itoh, M., and Toda, M. (1995). Immunologic self-tolerance maintained by activated T cells expressing IL-2 receptor alpha-chains (CD25). Breakdown of a single mechanism of self-tolerance causes various autoimmune diseases. J. Immunol. *155*, 1151–1164.

Savage, P.A., and Davis, M.M. (2001). A kinetic window constricts the T cell receptor repertoire in the thymus. Immunity *14*, 243–252.

Savage, P.A., Boniface, J.J., and Davis, M.M. (1999). A kinetic basis for T cell receptor repertoire selection during an immune response. Immunity *10*, 485–492.

Schlueter, A.J., Malek, T.R., Hostetler, C.N., Smith, P.A., deVries, P., and Waldschmidt, T.J. (1997). Distribution of Ly-6C on lymphocyte subsets: I. Influence of allotype on T lymphocyte expression. J. Immunol. *158*, 4211–4222.

Scollay, R., and Godfrey, D.I. (1995). Thymic emigration: conveyor belts or lucky dips? Immunol. Today *16*, 268–273; discussion 273–274.

Shapiro-Shelef, M., Lin, K.I., McHeyzer-Williams, L.J., Liao, J., McHeyzer-Williams, M.G., and Calame, K. (2003). Blimp-1 is required for the formation of immunoglobulin secreting plasma cells and pre-plasma memory B cells. Immunity *19*, 607–620.

Spangrude, G.J., Heimfeld, S., and Weissman, I.L. (1988). Purification and characterization of mouse hematopoietic stem cells. Science *241*, 58–62.

Tough, D.F., Borrow, P., and Sprent, J. (1996). Induction of bystander T cell proliferation by viruses and type I interferon in vivo. Science *272*, 1947–1950.

Walunas, T.L., Bruce, D.S., Dustin, L., Loh, D.Y., and Bluestone, J.A. (1995). Ly-6C is a marker of memory CD8+ T cells. J. Immunol. *155*, 1873–1883.

Woodland, D.L., and Dutton, R.W. (2003). Heterogeneity of CD4(+) and CD8(+) T cells. Curr. Opin. Immunol. *15*, 336–342.